RSC Advances

ROYAL SOCIETY OF CHEMISTRY

www.rsc.org/advances

Graphical Abstract

Manuscript title: A new polymorph $Cd_3B_2O_6$: synthesis, crystal structure and phase transformation

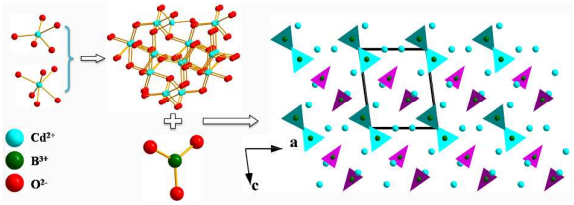

A new high-temperature phase of $Cd_3B_2O_6$ (β-$Cd_3B_2O_6$) has been discovered and the phase transformation process between α- and β-$Cd_3B_2O_6$ was investigated.

Journal Name

RSCPublishing

ARTICLE

A new polymorph $Cd_3B_2O_6$: synthesis, crystal structure and phase transformation

Cite this: DOI: 10.1039/x0xx00000x

Xingwen Zhang,[a,b] Hongwei Yu,[a,b] Hongping Wu,[*a] Shilie Pan,[*a] Anqing Jiao,[a,b] Bingbing Zhang,[a,b] Zhihua Yang[a]

Received 00th January 2012,
Accepted 00th January 2012

DOI: 10.1039/x0xx00000x

www.rsc.org/

A new polymorph of $Cd_3B_2O_6$ (β-$Cd_3B_2O_6$) has been grown through spontaneous crystallization with the flux system. β-$Cd_3B_2O_6$ crystallizes in triclinic space group $P\bar{1}$ and features a three-dimensional Cd−O network composed of CdO_n (n = 5, 6) distorted polyhedra and isolated planar BO_3 groups. The phase transformation of $Cd_3B_2O_6$ has been studied by the structure analysis and powder X-ray diffraction. TG-DSC measurement reveals the melting behavior and phase transformation temperature. Furthermore, IR spectrum was measured. The detailed structure comparison between $Cd_3B_2O_6$ and other cadmium-containing borates, such as CdB_4O_7, CdB_2O_4 and $Cd_2B_2O_5$ was also carried out.

Introduction

Polymorphism, the ability for a substance to adopt several distinct crystalline phases of identical composition, is observed for a variety of materials.[1] This phenomenon has become increasingly important and is attracting more attention because of the promising applications in pharmaceuticals, pigments, foods, dyestuffs and so forth.[2] Industrially, disastrous consequences can be speculated by a sudden unexplained switch of polymorph. Technologically, the structural variants exhibit different physical properties reflecting in optical characteristics, chemical reactivity, crystal morphology, etc.[3] α- and β-ZnS give a good example that the two polymorphs belong to different crystal systems and thus own different physical properties, which make them to possess different applications in nano materials and semiconductor materials.[4] Understanding polymorphism is valuable for the research of structure-property relationships. Extensive polymorphism has been reported in many inorganic materials, such as α-$BaTeMo_2O_9$[5] and β-$BaTeMo_2O_9$,[6] α-$Cs_2I_4O_{11}$[7] and β-$Cs_2I_4O_{11}$,[8] α-$KMoO_3(IO_3)$[9] and β-$KMoO_3(IO_3)$.[10]
In the study, we mainly focus on the borate polymorphs because they possess rich chemistry structures, generally, the B atoms can be coordinated by either three or four O atoms to form a BO_3 triangle or BO_4 tetrahedron, which can be further linked by sharing O atoms to form isolated rings and cages or to construct infinite chains, sheets, or networks. The rich structure chemistry of borates favors them to exhibit the phenomenon of polymorphs, which make borates ideal candidates for the research of the phase transformation. In addition, borates also exhibit many attractive properties such as efficient frequency conversion capability in nonlinear optical crystals, high electrical conductivity in ion conductors, and large birefringence in controlling the polarization of illuminating lasers.[11] And borate polymorphs with different crystal structures exhibit different physical properties and thus possess different applications. For example, BaB_2O_4 has two polymorphs with different space groups and distinct crystal structures. The low-temperature phase (β-BaB_2O_4) is a widely used nonlinear optical material, while the high-temperature phase (α-BaB_2O_4) also has excellent property for its large birefringence.[12]
In this work, a new $Cd_3B_2O_6$ phase was found in CdO-B_2O_3 system, it crystallizes in triclinic space group $P\bar{1}$. The other phase $Cd_3B_2O_6$ has been reported.[13] According to their crystallization temperature from low to high, the new $Cd_3B_2O_6$ phase can be regarded as the high-temperature phase β-$Cd_3B_2O_6$. TG-DSC of α-$Cd_3B_2O_6$ and IR spectra of α- and β-$Cd_3B_2O_6$ were measured. Furthermore, to better understand the phase transformation of $Cd_3B_2O_6$, polycrystalline samples of β-$Cd_3B_2O_6$ were synthesized by traditional solid-state reaction techniques at different reaction temperatures. The detailed comparison between $Cd_3B_2O_6$ and other cadmium-containing borates, such as CdB_4O_7, CdB_2O_4 and $Cd_2B_2O_5$ was also carried out.[14]

Experimental

Reagents

CdO (99%, Sinopharm Chemical Reagent Co., Ltd.) and H_3BO_3 (99%, Sinopharm Chemical Reagent Co., Ltd.) were used as received.

Crystal Growth

Small single crystals were grown from a high-temperature solution with the PbO-MoO_3 flux system in air. A mixture of raw materials CdO-H_3BO_3-PbO-MoO_3 with molar ratio 3.3: 2: 1: 1 was loaded in a platinum crucible and heated in a muffle furnace at 700 ℃ until the solution became transparent and clear. The homogenized solution was then cooled quickly (20 ℃/h) to the crystallization temperature (580 ℃), then slowly cooled (3 ℃/h) to 500 ℃, followed by cooling to room temperature after the furnace was powered off. Small colorless crystals of β-$Cd_3B_2O_6$ were obtained.

X-ray Crystallography

A colorless and transparent plate crystal of β-$Cd_3B_2O_6$ with dimensions of $0.063 \times 0.128 \times 0.161$ mm^3 was selected and mounted on a thin glass fiber of the Bruker SMART APEX II CCD diffractometer. Data were collected using monochromatic Mo Kα radiation (λ = 0.71073 Å) at 296(2) K and integrated with the SAINT program.[15] All calculations were performed with programs

from the SHELXTL crystallographic software package.[16] The structure was solved by direct methods using SHELXS-97.[17] The final full-matrix least-squares refinement was on F_o^2 with data having $F_o^2 \geq 2\sigma(F_o^2)$ and all of the atoms were refined with anisotropic thermal parameters. The final refinement was converged with $R_1 = 0.0149$ and $wR_2 = 0.0435$. The β-$Cd_3B_2O_6$ structure was checked for missing symmetry elements with *PLATON*.[18] The crystal data and structure refinement for β-$Cd_3B_2O_6$ are presented in Table 1. The atomic coordinates, related anisotropic displacement parameters, the bond valence calculation[19] for all atoms and selected bond lengths (Å) and angles (deg.) are summarized in Tables S1−S3 in the Supporting Information. The results of bond valence calculations (Cd, 1.93-2.08; B, 2.90-2.92) indicate that the Cd and B atoms are in oxidation states of +2 and +3, respectively.

Table 1. Crystal data and structure refinement for β-$Cd_3B_2O_6$.

Empirical formula	β-$Cd_3B_2O_6$
Formula weight	454.82
Crystal system	Triclinic
Space group, Z	$P\bar{1}$, 2
Unit cell dimensions	a = 6.1114(5) Å
	b = 6.1463(5) Å
	c = 7.4232(6) Å
	α= 76.521(3) °
	β= 80.730(3) °
	γ= 82.461(3) °
Volume	266.34(4) Å^3
Density (calculated)	5.671 Mg/m^3
Theta range for data collection	2.85° to 27.59°
Limiting indices	-7≤ h ≤7, -8≤ k ≤8, -9≤ l ≤9
Reflections collected / unique	3827 / 1205 [R(int) = 0.0194]
Completeness to theta	98.1 %
Goodness-of-fit on F^2	1.189
Final R indices [$F_o^2>2\sigma(F_o^2)$][a]	$R1$ = 0.0149, $wR2$ = 0.0435
R indices (all data)[a]	$R1$ = 0.0157, $wR2$ = 0.0439
Extinction coefficient	0.0213(9)
Largest diff. peak and hole (e Å^{-3})	0.955 and -0.674 e Å^{-3}

[a]$R_1 = \Sigma||F_o| - |F_c||/\Sigma|F_o|$ and $wR_2 = [\Sigma w(F_o^2 - F_c^2)^2/\Sigma wF_o^4]^{1/2}$ for $F_o^2 > 2\sigma(F_o^2)$

Powder X-ray Diffraction

Powder X-ray diffraction (XRD) analysis of β-$Cd_3B_2O_6$ was performed in flat plate at room temperature in the angular range of $10° < 2\theta < 70°$ with a scan step width of 0.02° and fixed counting time of 1 s/step with a Bruker D8 ADVANCE X-ray diffractometer with graphite monochromatized Cu Kα (λ = 1.5418 Å) radiation.

Thermal Analysis

Thermal analysis was carried out on a simultaneous NETZSCH STA 449C thermal analyzer instrument with a heating rate of 5 ℃/min. The measurement range extended from 35 to 1200 ℃ in an atmosphere of flowing N_2.

IR Spectroscopy

The IR absorption spectra were recorded on a Shimadzu IR Affinity-1 Fourier transform IR spectrometer to analyze the presence of functional groups in the α- and β-$Cd_3B_2O_6$ compounds. The samples were mixed thoroughly with dried KBr (1 mg of the sample, 100 mg of KBr). The spectra were collected in the range from 400 to 4000 cm^{-1} with a resolution of 2 cm^{-1}.

Results and discussion

Synthesis and Phase Transformation

Polycrystalline samples of β-$Cd_3B_2O_6$ were synthesized by traditional solid-state reaction techniques. Pure polycrystalline β-$Cd_3B_2O_6$ was not obtained, even with different proportions of raw materials and various dwell times at temperature. For example, superfluous CdO was also tried owing to its high vapor pressure. However, the experimental results were still unsatisfied. The polycrystalline β-$Cd_3B_2O_6$ was always mixed with some α-$Cd_3B_2O_6$, while pure polycrystalline α-$Cd_3B_2O_6$ has been obtained easily. To investigate the phase transformation, TG-DSC of pure α-$Cd_3B_2O_6$ was measured as shown in Figure 1. The DSC curve exhibits two endothermic peaks at 862 and 985 ℃ upon heating to 1200 ℃. There is weight loss on the TG curve from 985 ℃. 862 and 985 ℃ are the phase transformation temperature and melting temperature, respectively. For confirmation of this and investigation of its phase transformation, a series of experiments at different reaction temperatures (850-1000 ℃) were conducted. Stoichiometric mixture

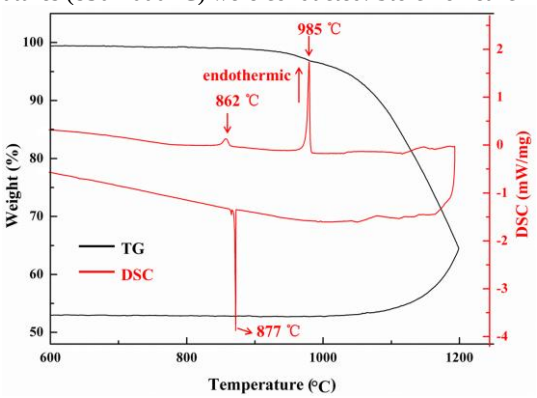

Figure 1 TG-DSC curves of α-$Cd_3B_2O_6$.

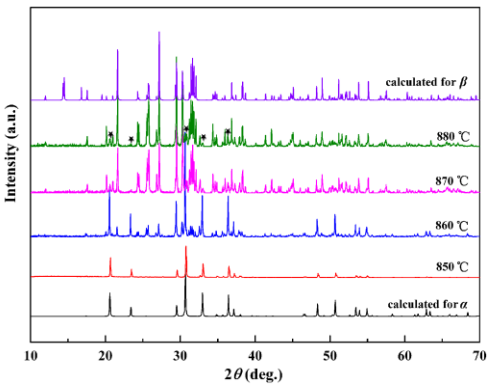

Figure 2 Powder XRD traces showing the influence of reaction temperature on polymorph formation. Denotation ★ represents the α-$Cd_3B_2O_6$ crystalline phase.

of CdO and H_3BO_3 were thoroughly ground in an agate mortar and then packed into a platinum crucible. The crucible was heated in air from room temperature to 850 ℃ at a rate of 20 ℃/min and allowed to dwell at the temperature for 24 h, grounded three times during the sintered process, and then quenched in air. The phase purity of the resultant solid was confirmed by powder XRD. When the temperatures were higher than 880 ℃, the powder XRD patterns were similar. Then, the XRD patterns at 850-880 ℃ are shown in Figure 2. As shown in Figure 2, the phase transformation begins at about 860 ℃. When the temperature was raised to 1000 ℃, the powders melted. The result is consistent with our previous prediction that 862 ℃ and 985 ℃ are the phase transformation temperature and melting temperature of β-$Cd_3B_2O_6$, respectively.

In order to further research the phase transformation of $Cd_3B_2O_6$, the sample after melting has been characterized by the powder XRD. The powder of β-$Cd_3B_2O_6$ melt at 1000 ℃ for 10 h, the different cooling rates of melt were explored. For Sample 1 in Figure 3, the temperature decreased from 1000 to 800 °C at a rate of 2 °C/h, and allowed to cool to room temperature after the furnace was turned off. Powder XRD revealed that the main product was α-$Cd_3B_2O_6$ with some β-$Cd_3B_2O_6$. For Sample 2, the melting β-$Cd_3B_2O_6$ powder was directly quenched in ice-water mixture. Powder XRD revealed that the main product was β-$Cd_3B_2O_6$ with some α-$Cd_3B_2O_6$. The above results indicate that β-$Cd_3B_2O_6$ is a congruent melting compound and the energy barrier from β-$Cd_3B_2O_6$ to α-$Cd_3B_2O_6$ is very low. Hence, the crystallized β-$Cd_3B_2O_6$ products always include some α-$Cd_3B_2O_6$ and the pure polycrystalline β-$Cd_3B_2O_6$ is difficult to obtain. In addition, the before and after melting XRD patterns also indicate that the weight loss on the TG curve was just due to the volatilization.

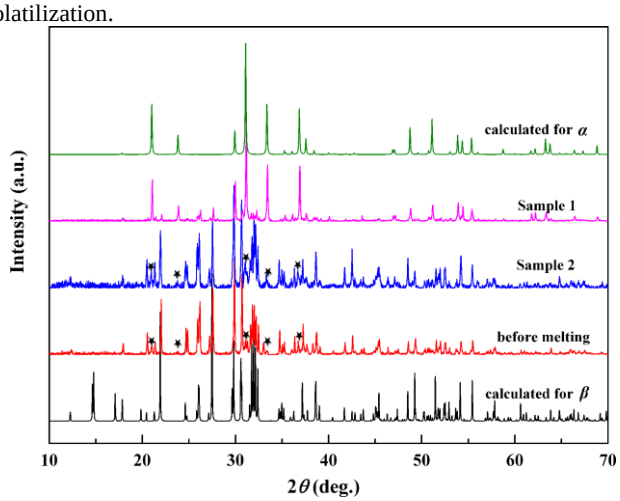

Figure 3 Calculated XRD patterns of α- and β-$Cd_3B_2O_6$ and the before and after melting XRD patterns of β-$Cd_3B_2O_6$. Lines 1 and 2 represent the after melting XRD patterns. Line 1 represents the result that adopts the slow decreasing temperature program while line 2 is the result of quenching experiment. Denotation ★ represents the α-$Cd_3B_2O_6$ crystalline phase.

Structural Description

β-$Cd_3B_2O_6$ crystallizes in the centrosymmetric triclinic system with space group $P\bar{1}$, and its structure is illustrated in Figure 4. β-$Cd_3B_2O_6$ features a three-dimensional (3D) Cd−O network composed of CdO_n (n = 5, 6) distorted polyhedra and isolated planar BO_3 groups. In the asymmetric unit, Cd, B, and O each occupy three, two, and six crystallographically unique positions, respectively. In the CdO_n (n = 5, 6) polyhedra, the bond lengths vary from 2.143(2) to 2.424(2) Å, with O−Cd−O bond angles from 59.43(8)° to 173.31(8)°. In the BO_3 triangles, the bond lengths and angles range from 1.366(4) to 1.391(4) Å and from 116.4(3) ° to 123.4(3) °, respectively. The mean bond length in the BO_3 triangle is 1.383 Å. These bond lengths and angles in β-$Cd_3B_2O_6$ are comparable with those reported in other borates.[20]

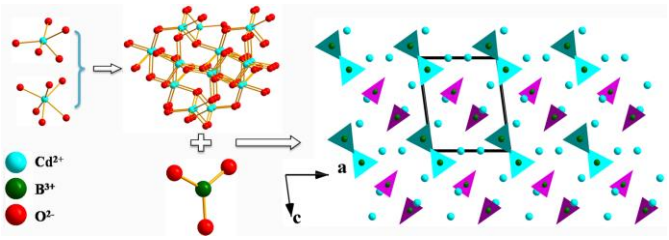

Figure 4 View of the β-$Cd_3B_2O_6$ crystal structure along the *b*-axis. $B1O_3$ and $B2O_3$ groups are shown in pink and blue, respectively. The bonds of Cd–O are removed for clarity.

In β-$Cd_3B_2O_6$, there are three unique Cd-O polyhedra: $Cd1O_6$, $Cd2O_5$, $Cd3O_6$. These CdO_n (n = 5, 6) polyhedra are linked through common corners and edges to form a 3D framework. Among Cd-O groups, each Cd1-centered octahedron shares corners with two Cd2-centered hexahedra and four Cd3-centered octahedra and simultaneously shares one edge with two Cd1 and one Cd3-centered octahedra. Each Cd2-centered hexahedron shares corners with two Cd1-centered octahedra and three Cd3-centered octahedra and shares one edge with two Cd2-centered hexahedra. Each Cd3-centered octahedron is linked with four Cd1-centered octahedra and three Cd2-centered hexahedra and shares one edge with one Cd1 and one Cd3-centered octahedra (Figure S1 in the Supporting Information). The Cd ··Cd distances of two adjacent Cd-O polyhedra contacted across the shared edges (the average is 3.3917Å) are markedly shorter than those associated with shared corners (the average is 3.9273 Å), and the O–Cd–O angles in the Cd-O polyhedron contacted across the shared edges (the average is 82.644 °) are also significantly smaller than those associated with shared corners (the average is 109.57 °) due to the constraint of the Cd–O–Cd–O four-membered rings (Figure S1 and Table S3 in the Supporting Information).

Two adjacent isolated planar $B1O_3$ and $B2O_3$ groups are parallel to each other with totally opposite orientation, respectively. Each $B1O_3$ triangle shares its three vertices with six neighboring CdO_6 octahedra and two CdO_5 hexahedra, while each $B2O_3$ triangle shares its three vertices with four neighboring CdO_6 octahedra and three CdO_5 hexahedra (Figure S1 in the Supporting Information). It is also worth noting that each BO_3 triangle shares its one edge with neighboring CdO_6 octahedra developing Cd–O–B–O four-membered rings which lead to distinct small O-Cd-O angles. As mentioned above, Cd–O–Cd–O and Cd–O–B–O four-membered rings are

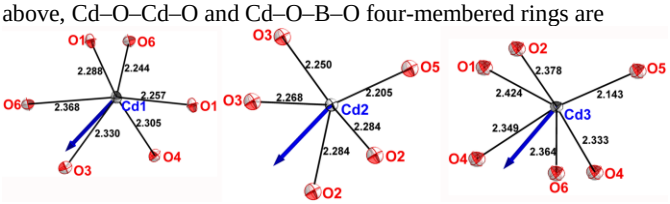

Figure 5 The approximate directions of the dipole moments for CdO_n (n = 5, 6) polyhedra in β-$Cd_3B_2O_6$. The unit of Cd-O bond length is Å.

responsible for the highly distorted CdO_n (n = 5, 6) polyhedra. To better understand the distortion of the CdO_n (n = 5, 6) polyhedra, we further calculated their dipole moments by the simple valence method.[21] The approximate directions of the dipole moments for CdO_n (n = 5, 6) polyhedra are shown in Figure 5 and the magnitudes of dipole moments of CdO_n (n = 5, 6) polyhedra in α- and β-

$Cd_3B_2O_6$ are shown in Table S4 in the Supporting Information. The result reveals that the distortions of CdO_n (n = 5, 6) polyhedra in β-$Cd_3B_2O_6$ are larger than those in α-$Cd_3B_2O_6$.

Comparing the Structures with α-$Cd_3B_2O_6$

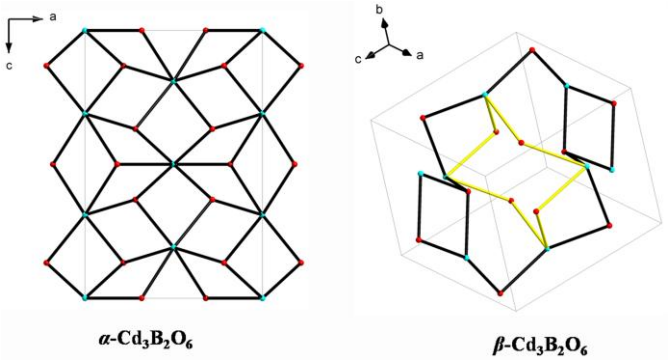

Figure 6 The Cd-O frameworks in α- and β-$Cd_3B_2O_6$. The yellow Cd-O bonds represent the eight-membered rings emerged in β-$Cd_3B_2O_6$. The BO_3 groups are removed for clarity.

To further well understand the structure of β-$Cd_3B_2O_6$, we compared the structures between the two phases in detail. The structure of α-$Cd_3B_2O_6$ is built up of a 3D Cd−O network composed of solely CdO_6 distorted polyhedra and isolated planar BO_3 groups.[13] The different orientation of the BO_3 groups and the variation of the connection modes of Cd-O groups contribute for the structural versatility of $Cd_3B_2O_6$. It is worth noting that in α- and β-$Cd_3B_2O_6$, the Cd-O frameworks both consist of the Cd-O four- and six-membered rings, however, the ratio of four-membered rings in α-$Cd_3B_2O_6$ is higher than that in β-$Cd_3B_2O_6$. And in β-$Cd_3B_2O_6$, the large eight-membered rings are observed, as shown in Figure 6. In addition, in β-$Cd_3B_2O_6$, two kinds of Cd-O coordination-sphere (CdO_5, CdO_6) are observed, while only one kind of CdO_6 octahedra is observed in α-$Cd_3B_2O_6$. The different structural features could cause the loose structure of β-$Cd_3B_2O_6$ when compared with α-$Cd_3B_2O_6$. Based on the calculated densities, β-$Cd_3B_2O_6$ is 5.671 g/cm^3, while α-$Cd_3B_2O_6$ is 5.870 g/cm^3. The result is consistent with above structure analysis. We think that the higher crystallization temperature of β-$Cd_3B_2O_6$ results in more vigorous atomic thermal motion, which further drives the formation of different loose Cd-O framework and realizes the phase transition.

Other Cadmium-containing Borates

A further crystal structure research was performed on other cadmium-containing borates to investigate the reason of the formation of different $Cd_3B_2O_6$ polymorphs. CdB_4O_7, CdB_2O_4, $Cd_2B_2O_5$, α-$Cd_3B_2O_6$ and β-$Cd_3B_2O_6$ can be written as CdO $2B_2O_3$ and xCdO B_2O_3 (x = 1, 2, 3) to reflect the rising proportion of Cd^{2+} cations. There are rule changes in the connecting patterns of B-O groups. As shown in Figure 7, when Cd/B < 1 (in CdO $2B_2O_3$, Cd/B = 0.25 and in CdO B_2O_3, Cd/B = 0.5), the B-O groups include BO_3 triangles or BO_4 tetrahedra, which can be further linked by sharing O atoms to form 3D networks. When Cd/B = 1 (in 2CdO B_2O_3), two BO_3 triangles sharing one O atom form the B_2O_5 unit. When Cd/B > 1 (in α- and β-$Cd_3B_2O_6$, Cd/B = 1.5), B and O atoms only form the isolated BO_3 triangles. We think that the solely isolated BO_3 triangles possess more flexible arrangement modes which further contribute to the formation of different $Cd_3B_2O_6$ polymorphs. Moreover, it might appear isolated BO_4 tetrahedra or O^{2-} ions which are not linked to B atoms when the Cd/B ratio is increased higher than 1.5. This conclusion will give a meaningful guide to ensuing experiments in CdO-B_2O_3 system.

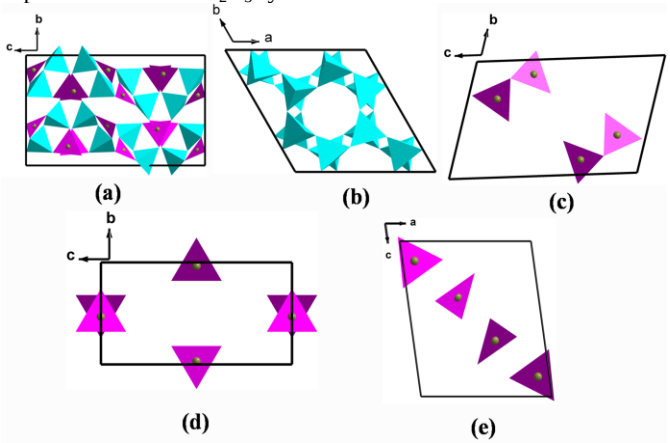

Figure 7 The B-O groups in CdO $2B_2O_3$ (a), CdO B_2O_3 (b), 2CdO B_2O_3 (c), α-3CdO B_2O_3 (d), β-3CdO B_2O_3 (e). BO_4 tetrahedra and BO_3 triangles are shown in blue and pink, respectively.

IR Spectroscopy

IR spectra of α- and β-$Cd_3B_2O_6$ are presented in Figure S2 in the Supporting Information and they are similar. Referring to the literatures,[22] the peaks at 1453, 1267, and 1106 cm^{-1} for α-$Cd_3B_2O_6$, 1438, 1202, and 1154 cm^{-1} for β-$Cd_3B_2O_6$ can be assigned to the asymmetric stretching and symmetric stretching vibrations of BO_3, while the peaks located at 804, 697 and 612 cm^{-1} for α-$Cd_3B_2O_6$, 877, 709 and 615 cm^{-1} for β-$Cd_3B_2O_6$ are likely to be from the out-of-plane bending of B–O in BO_3, respectively. The peaks at 568 cm^{-1} for α-$Cd_3B_2O_6$, 580 and 508 cm^{-1} for β-$Cd_3B_2O_6$ are attributed to bending vibrations. IR spectra indicate that only BO_3 groups are included in α- and β-$Cd_3B_2O_6$.

Conclusion

A new high-temperature phase of $Cd_3B_2O_6$, namely, β-$Cd_3B_2O_6$, has been discovered. It crystallizes in the triclinic space group $P\bar{1}$, and displays a 3D framework composed of CdO_n (n = 5, 6) distorted polyhedra and isolated BO_3 groups. The phase transformation process between α- and β-$Cd_3B_2O_6$ was presented and their crystal structures were compared. TG-DSC and polycrystalline samples synthesis of β-$Cd_3B_2O_6$ at different reaction temperatures by traditional solid-state reaction techniques reveal that 862 and 985 ℃ are the phase transformation temperature and melting temperature, respectively. IR spectra of α- and β-$Cd_3B_2O_6$ indicate that only BO_3 groups are included in the two polymorphs. Furthermore, the crystal structures of other cadmium-containing borates have also been discussed to understand the formation of different $Cd_3B_2O_6$ polymorphs. We think that the solely isolated BO_3 triangles, which possess more flexible arrangement modes, contribute to the formation of different $Cd_3B_2O_6$ polymorphs. Our future research efforts will be devoted to exploring other borate polymorphs.

Acknowledgements

This work is supported by the High Technology Research & Development Program of Xinjiang Uygur Autonomous Region of China (Grant Nos. 201315103, 201116143), 973 Program of China (Grant Nos. 2014CB648400, 2012CB626803), the National Natural Science Foundation of China (Grant Nos. 21201176, U1129301, U1303392, 51172277, 51202287), the Western Light Program of CAS (Grant No.XBBS201214), Main Direction Program of Knowledge Innovation of CAS

(Grant No. KJCX2-EW-H03-03) and the Science and Technology Project of Urumqi (Grant No. G121130002).

Notes and references

[a] Key Laboratory of Functional Materials and Devices for Special Environments of CAS; Xinjiang Key Laboratory of Electronic Information Materials and Devices; Xinjiang Technical Institute of Physics & Chemistry of CAS, 40-1 South Beijing Road, Urumqi 830011, China. E-mail: wuhp@ms.xjb.ac.cn (Hongping Wu); slpan@ms.xjb.ac.cn (Shilie Pan)

[b] University of Chinese Academy of Sciences, Beijing 100049, China.

Fax: (86)-991-3838957; Tel: (86)-991-3674558.

† Electronic Supplementary Information (ESI) available: ICSD-number 427222 for β-$Cd_3B_2O_6$ Crystal data (CIF file); Checkcif; Atomic coordinates, related anisotropic displacement parameters, the bond valence calculation for all atoms; selected bond lengths (Å) and angles (deg.); coordinated environments of the Cd and B atoms in β-$Cd_3B_2O_6$; IR spectra of α- and β-$Cd_3B_2O_6$. See DOI: 10.1039/b000000x/

1 W. C. McCrone, *Phys. Chem. Org. Solid State* 1965, **2**, 725.

2 (a) W. H. Streng, *Drug Discov. Today* 1997, **2**, 415. (b) S. R. Vippagunta, H. G. Brittain, D. J. W. Grant, *Adv. Drug. Delivery. Rev.* 2001, **48**, 3. (c) H. G. Brittain, *J. Pharm. Sci*. 2007, **96**, 705.

3 (a) J. Bernstein, *Org. Solid State Chem.* 1987, **32**, 471. (b) P. H. v. Groth, *Chemische Kristallographie*; Wilhelm Engelmann: Leipzig, 1917; Vol. **4**. (c) P. H. v. Groth, *Chemische Kristallographie*; Wilhelm Engelmann: Leipzig, 1919; Vol. **5**.

4 E. Monroy, F. Omnes, F. Calle, *Semicond. Sci. Technol.* 2003, **18**, R33.

5 J. J. Zhang, Z. H. Zhang, W. G. Zhang, Q. X. Zheng, Y. X. Sun, C. Q. Zhang, X. T. Tao, *Chem. Mater.* 2011, **23**, 3752.

6 W. G. Zhang, X. T. Tao, C. Q. Zhang, H. J. Zhang, M. H. Jiang, *Cryst. Growth Des.* 2009, **9**, 263.

7 K. M. Ok, P. S. Halasyamani, *Angew.Chem. Int. Ed*. 2004, **43**, 5489.

8 K. M. Ok, P. S. Halasyamani, *Inorg. Chem.* 2005, **44**, 9353.

9 R. E. Sykora, K. M. Ok, P. S. Halasyamani, T. E. Albrecht-Schmitt, *J. Am. Chem. Soc*. 2002, **124**, 1951.

10 R. E. Sykora, D. M. Wells, T. E. Albrecht-Schmitt, *J. Solid State Chem.* 2002, **166**, 442.

11 (a) H. P. Wu, H. W. Yu, S. L. Pan, Z. J. Huang, Z. H. Yang, X. Su, Kenneth R. Poeppelmeier, *Angew. Chem. Int. Ed*. 2013, **52**, 3406. (b) H. P. Wu, H. W. Yu, Z. H. Yang, X. L. Hou, S. L. Pan, X. Su, K. R. Poeppelmeier, J. M. Rondinelli, *J. Am. Chem. Soc*. 2013, **135**, 4215.

12 (a) C. T. Chen, Y. C. Wu, A. D. Jiang, B. C. Wu, G. M. You, *Sci. Sin. B* 1985, **28**, 235. (b) S. F. Wu, G. F. Wang, J. L. Xie, X. Q. Wu, Y. F. Zhang, X. Lin, *J. Cryst. Growth* 2002, **245**, 84.

13 Y. H. Zhao, X. A. Chen, X. A. Chang, J. L. Zuo, M. Li, *Acta Crystallogr*. 2007, **E63**, i50.

14 (a) M. Ihara, J. Krogh-Moe, *Acta Crystallogr*. 1966, **20**, 132. (b) M. Weil, *Acta Crystallogr.* 2003, **E59**, i95. (c) J. S. Knyrim, H. Emme, M. Döblinger, O. Oeckler, M. Weil, H. Huppertz, *Chem. Eur. J.* 2008, **14**, 6149.

15 *SAINT-Plus*, version 6.02A; Bruker Analytical X-ray Instruments, Inc.: Madison, WI, 2000.

16 G. M. Sheldrick, SHELXTL, version 6.14; Bruker Analytical X-ray Instruments, Inc.: Madison, WI, 2003.

17 G. M. Sheldrick, SHELXS-97, Program for X-ray Crystal Structure Solution; University of Göttingen: Göttingen, Germany, 1997.

18 A. L. Spek, *J. Appl. Crystallogr*. 2003, **36**, 7.

19 (a) N.E. Brese, M. Okeeffe, *Acta Crystallogr.* B 1991, **47**, 192. (b) I. D.Brown, D. Altermatt, *Acta Crystallogr*. B 1985, **41**, 244.

20 (a) C. T. Chen, Y. B. Wang, Y. N. Xia, B. C. Wu, D. Y. Tang, K. C. Wu, W. R. Zeng, L. H. Yu, *J. Appl. Phys.* 1995, **77**, 2268. (b) H. W. Huang, J. Y. Yao, Z. S. Lin, X. Y. Wang, R. He, W. J. Yao, N. X. Zhai, C. T. Chen, *Angew. Chem. Int. Ed*. 2011, **50**, 9141.

21 P. S. Halasyamani, *Chem. Mater.* 2004, **16**, 3586.

22 (a) Y. Yang, S. L. Pan, J. Han, X. L. Hou, Z. X. Zhou, W. W. Zhao, Z. H. Chen, M. Zhang, *Cryst. Growth Des.* 2011, **11**, 3912. (b) L. Wang, S. L. Pan, L. X. Chang, J. Y. Hu, H. W. Yu, *Inorg. Chem.* 2012, **51** 1852. (c) Y. J. Wang, S. L. Pan, X. L. Tian, Z. X. Zhou, G. Liu, J. Wang, D. Z. Jia, *Inorg. Chem.* 2009, **48**, 7800.